Rev. Energ. Ren. Vol. 9 (2006) 17 - 28

Comparative study of photovoltaic pumping systems using a permanent magnet synchronous motor (PMSM) and an asynchronous motor (ASM)

R. Chenni*, L. Zarour†, A. Bouzid and T. Kerbache

Laboratoire d'Electrotechnique, Faculté des Sciences de l'Ingénieur
Université Mentouri, Constantine, Algérie

(reçu le 04/12/05; accepté le 07/02/06)

Abstract - *The dynamic performances of a permanent magnet synchronous motor (PMSM) and an asynchronous motor (ASM) connected to a photovoltaic (PV) array through an inverter are analyzed. The mathematical models of PV array, inverter/motor and controller are developed. The photovoltaic array is represented by an equivalent circuit whose parameters are computed using experimentally determined current-voltage I-V characteristics. The necessary computer algorithm is developed to analyze the performance under different conditions of the solar illumination for pump load. The study also examines the effectiveness of the drive system both for starting and DC link voltage fluctuations caused by varying solar illumination.*

Résumé - *Les performances dynamiques d'un moteur synchrone à aimant permanent (PMSM) et d'un moteur asynchrone (ASM) connecté à un générateur photovoltaïque (GPV) à travers un convertisseur sont analysés. Les modèles mathématiques du panneau photovoltaïque, de l'ensemble convertisseur moteur et du contrôleur sont développés. Le générateur photovoltaïque est représenté par un circuit équivalent dont les paramètres sont calculés expérimentalement en utilisant la caractéristique courant tension I-V. L'algorithme nécessaire est développé pour analyser la performance du groupe motopompe sous différentes conditions de l'éclairement solaire et de la température. L'étude teste également l'efficacité du système d'entraînement pendant le démarrage et pour des fluctuations de tension provoquées par le changement brusque de l'éclairement solaire.*

Key words: Solar energy - Optimization - Photovoltaic arrays - Pumping - Global efficiency.

1. INTRODUCTION

Several authors lent much attention to the study of the dynamic performance of the photovoltaic pumping systems. Appelbaum and Bany [1] analyzed the performance of a direct motor with separate excitation fed by a photovoltaic generator. Later, Appelbaum [2] studied the dynamic behaviour of a photovoltaic panel associated directly with a DC motor with excitation series. Roger [3] showed that a load such centrifugal pump, driven by a DC motor, represents a load matched to the characteristics of PV generator. In a former work, the dynamic performance of a PV generator involving a system, permanent magnet motor associate at a centrifugal pump, was studied by Anis and Metwally [4]. Recently Betka [5] presented the performance optimization of an asynchronous motor associated at a PV generator.

In this work, the dynamic performance of a system which uses, once a synchronous motor with permanent magnet and another time an asynchronous motor, is studied. For this last type of engine, the primary current and flux changes in accordance with the changes in the applied voltage. It is not the case with the permanent magnet synchronous motor where flux is constant. The electric model of the system is simulated using the software MATLAB 6p5 for various solar illuminations and temperatures.

2. ELECTRICAL MODEL FOR A PHOTOVOLTAIC CELL

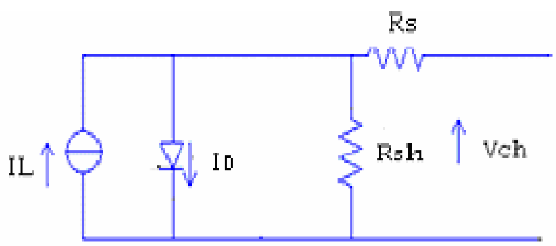

Fig. 1: Equivalent circuit of PV cell

* rachid.chenni@caramail.com
† laidzarour@hotmail.fr

The electrical model of a solar cell is composed of a diode, two resistances and a current generator [6 - 8]. The relationship between the voltage V (volts) and the current density I (ampere) is given by:

$$I = I_L - I_0 \left\{ \exp\left(\frac{V + R_S I}{A} \right) - 1 \right\} - \left(\frac{V + R_S I}{R_{Sh}} \right) \tag{1}$$

where: I_L, I_0 and I are the photocurrent, the inverse saturation current and the operating current, R_S and R_{Sh} are series and parallel resistances respectively, which depend on the incident solar radiation and the cell's temperature. $A = \frac{k\,T}{q}$ is the diode quality factor. k and q are Boltzmann's constant and electronic charge respectively. Townsend (1989), Eckstein (1990), Al-Ibrahimi (1996), propose the model with four parameters assuming that the parallel resistance is infinite. So the equation (1) can be rewritten.

$$I = I_L - I_0 \left\{ \exp\left(\frac{V + R_S I}{A} \right) - 1 \right\} \tag{2}$$

The current and the voltage parameters of the PV generator are: $I_{pv} = I$ and $V_{pv} = n_s\,.\,Ns\,.\,V$, where n_s, Ns are the number of series cells in panel and series panels in generator ($n_s = 36$).

Now only the four parameters I_L, I_0, R_S and A need to be evaluated, a method to calculate these parameters has been developed by Townsend (1989) and Eckstein (1990), Duffie and Beckman (1991). Since there are four unknown parameters, four conditions of the current I and the voltage V are needed. Generally, available manufacturer's information are set at three points at the reference conditions, $G = 1000\,W/m^2$ and $T = 25\,°C$, the voltage at open circuit $V_{oc,ref}$, the current at short circuit $I_{sc,ref}$ and the maximum power point $V_{mp,ref}$ and $I_{mp,ref}$.

The 4th condition comes from the knowledge of the temperature coefficient $\mu_{I_{sc}}$ at short circuit and $\mu_{V_{oc}}$ at open circuit. E_q is the band gap energy (1.12 eV).

Equations (3) to (6) are used to calculate these parameters of the photovoltaic cells in a standard condition based on the experimental data.

$$R_{S,ref} = \frac{A_{ref} \times \ln\left(1 - \frac{I_{mp,ref}}{I_{L,ref}} \right) - V_{mp,ref} + V_{oc,ref}}{I_{mp,ref}} \tag{3}$$

$$A = \frac{\mu_{V_{oc}} \times T_{c,ref} - V_{oc,ref} + E_q \times n_s}{\frac{T_{c,ref} \times \mu_{I_{sc}}}{I_{L,ref}} - 3} \tag{4}$$

From equation (2) at reference condition and short circuit point, the diode current I_0 is very small (in order to 10^{-5} at 10^{-6} A), so the exponential term is neglected.

$$I_{sc,ref} \cong I_{L,ref} \tag{5}$$

$$I_{0,ref} = \frac{I_{L,ref}}{\exp\left(\frac{V + R_S\,.\,I}{A} \right) - 1} \tag{6}$$

The indices oc, sc, mp and ref refer to the open circuit, the short circuit, the maximum power and the reference condition respectively. The cell's parameters change with the solar radiation $G\ (W/m^2)$ and ambient temperature $T(K)$ [7] and can be estimated by the following equation. For a given radiation and temperature, the cell's parameters are then calculated from:

$$T = T_a + \frac{G_T}{G_{T\,noct}}\left(T_{noct} - T_a\right)\left(1 - \frac{\eta_c}{\tau_\alpha}\right) \tag{7}$$

$$I_L = \left(\frac{G}{G_{ref}}\right)\left\{I_{L,ref} + \mu_{I_{sc}}\left(T_c - T_{ref}\right)\right\} \tag{8}$$

$$I_0 = I_{0,ref}\left(\frac{T}{T_{ref}}\right)^3 \exp\left\{\left(\frac{n_s E_q}{A}\right)\left(1 - \frac{T_{c,ref}}{T_c}\right)\right\} \tag{9}$$

$$R_S = R_{S,ref} \tag{10}$$

$$A = A_{ref} \times \frac{T_c}{T_{c,ref}} \tag{11}$$

where T_a: ambient temperature, η_c: cell efficiency, T_{noct}: nominal operating cell temperature and τ_α: transmittance absorbance product.

These four parameters, for ambient conditions, are found from the equations (7) to (11). By injecting these parameters in the equation (2), we obtain $I - V$ characteristics.

<u>**PV array characteristics**</u>: Ns = 11 panels in series; GTO136-80/2; AM = 1.5; $P_m = 80\,W$; $V_{oc,ref} = 21.5\ V$; $I_{sc} = 4.73\ A$; $I_{mp,ref} = 4.25\ A$; $V_{mp,ref} = 16.9\,A$; $T_{noct} = 45\,°C$; $G_{ref} = 1000\,W/m^2$; $T_{ref} = 298\,K$; $\mu_{I_{sc}} = 3\ 10^{-3}\ A/°C$; $\mu_{V_{oc}} = 82\ 10^{3}\ V/°C$.

3. GLOBAL SYSTEM MODELLING

The decomposition of the total system in elementary blocks is related directly to the physical function of the block.

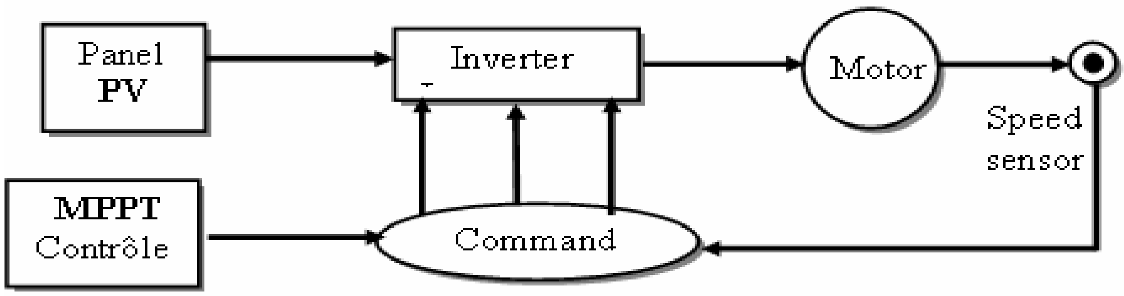

Fig. 2: Block diagram of the global system

3.1 PMSM electrical model

The model of the synchronous motor (PMSM) represented by the three fixed stator windings and the permanent magnet rotor is:

The mathematical dynamic model of a PMSMotor can be described by the following equations in a synchronously rotating d–q reference frame (Grellet and Clerc, 1997) [9]: where V_d and V_q, L_d and L_q, i_d and i_q are stator voltages, inductances, and currents components in the (d,q) axis respectively, R_a is the stator resistance per phase, ϕ_f is the rotor flux linkage due to the rotor permanent magnet frame, and p_p is the number of pole pairs.

Using the Park transformation, we pass from the real sizes $\left(V_a, V_b, V_c \text{ and } i_a, i_b, i_c\right)$ to their components $\left(V_o, V_d, V_q \text{ and } io, i_d, i_q\right)$.

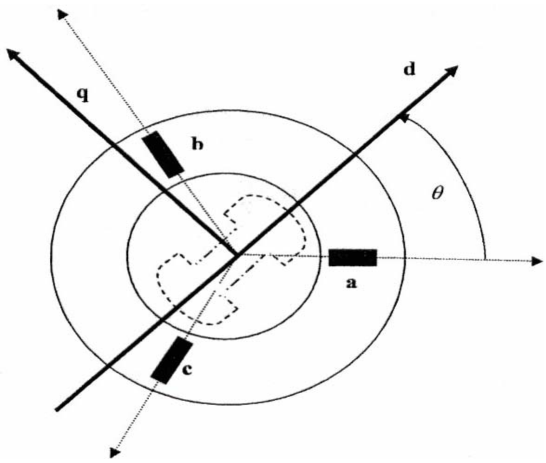

Fig. 3: PMSM three phase model

The Park matrix is expressed by [9]:

$$[P(\theta)] = \sqrt{\frac{2}{3}} \times \begin{bmatrix} \frac{1}{\sqrt{2}} & \cos\theta & -\sin\theta \\ \frac{1}{\sqrt{2}} & \cos\left(\theta - \frac{2\pi}{3}\right) & -\sin\left(\theta - \frac{2\pi}{3}\right) \\ \frac{1}{\sqrt{2}} & \cos\left(\theta - \frac{4\pi}{3}\right) & -\sin\left(\theta - \frac{4\pi}{3}\right) \end{bmatrix} \tag{12}$$

In matrix form:

$$\begin{bmatrix} V_d \\ V_q \end{bmatrix} = \begin{bmatrix} R_a & -L_q.\omega \\ L_d.\omega & R_a \end{bmatrix} \times \begin{bmatrix} i_d \\ i_q \end{bmatrix} + \begin{bmatrix} L_d & 0 \\ 0 & L_q \end{bmatrix} \times \frac{d}{dt} \begin{bmatrix} i_d \\ i_q \end{bmatrix} + \begin{bmatrix} 0 \\ \phi_f . \omega \end{bmatrix} \tag{13}$$

Moreover, the PMSM developed electromagnetic torque is given by the following equation:

$$C_{em} = \frac{1}{2} \cdot [i_s] \cdot \left\{ \frac{d}{d\theta_m} [L] \right\} \times [i_s] \tag{14}$$

with : $\theta_e = \theta_m \times p_P$

θ_e , θ_m the electrical angle and mechanical respectively, and the electromagnetic torque is:

$$C_{em} = p_P \times \left[(L_d - L_q) \times i_d + \phi_f \right] \times i_q \tag{15}$$

For a synchronous machine with smooth poles $(L_d = L_q)$, the torque will be $C_{em} = p_P . \phi_f . i_q$. The mechanical equation is written:

$$J \frac{d\omega}{dt} + f\omega = C_{em} - C_r \tag{16}$$

where, f and C_r are the friction coefficient and the resistant torque respectively.

PMS Motor's Characteristics: $P = 746$ W ; $\omega = 188.95$ rad/sec ; $V = 208$ V ; $I_s = 3$ A ; $I_{sn} = 5$ A ; $f = 60$ Hz ; $R_a = 1.93\ \Omega$ $L_d = 0.042$ H ; $\psi = 0.003$ Wb ; $J = 3\ 10^{-3}$ kg/m^2 ; $p_p = 2$.

PI parameters: For speed: $T_i = 0.01$; $K_p = 1$. For current: $T_i = 10$; $K_p = 5$.

3.2 Voltage source inverter model

For a three phase equilibrated system, we have: $(V_{an} + V_{bn} + V_{cn} = 0)$ and $(V_{1m} + V_{2m} + V_{3m} = 3\ V_{nm})$. In matrix form:

$$\begin{bmatrix} V_{an} \\ V_{bn} \\ V_{cn} \end{bmatrix} = \begin{bmatrix} \frac{2}{3} & -\frac{1}{3} & -\frac{1}{3} \\ -\frac{1}{3} & \frac{2}{3} & -\frac{1}{3} \\ -\frac{1}{3} & -\frac{1}{3} & \frac{2}{3} \end{bmatrix} \times \left[V_{pv} \right] \tag{17}$$

V_{pv} is photovoltaic generator voltage.

4. VECTORIAL COMMAND PRINCIPLE

From the equation (15), the torque control is made on the components of current i_d and i_q. The electromagnetic torque depends only on component i_q. It is maximum for a given current if we impose $i_d = 0$. The obtained torque is then proportional to the current of the machine power supply as in the case of a separately excited DC motor:

$$C_{em} = p_p \times \phi_f \times i_q .$$

5. REGULATORS

To optimize the system with given performances, the system must be controlled. The first role of a regulation system is to oblige the controlled parameters (output of the system) to preserve values as close as possible as those which one chooses like references values. Generally the control devices are with closed loop. For this command, there are three correctors PI used to control the speed and the two components of the stator current. The closed speed loop can be represented by the Fig. 4. This transfer function in closed loop has a dynamics of 2^{nd} order. By identifying the denominator with the canonical form $\dfrac{1}{1+\dfrac{2\xi}{\omega_n}p+\dfrac{p^2}{\omega_n^2}}$, we obtain:

$$\frac{J}{Ki} = \frac{1}{\omega_n^2} \tag{18}$$

$$\frac{2\xi}{\omega_n} = \frac{Kp + f}{Ki} \tag{19}$$

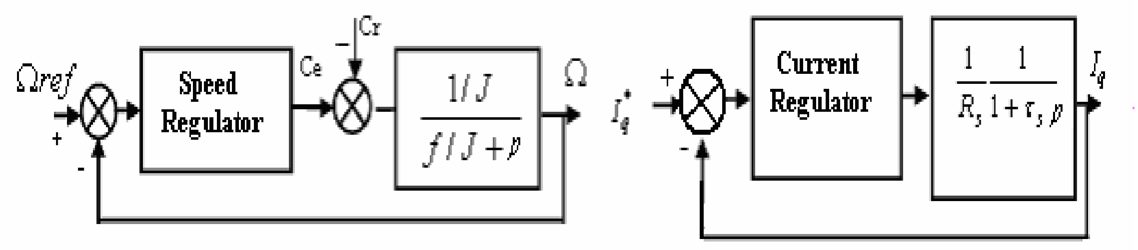

Fig. 4: Block diagram of the speed and current regulators

6. DESCRIPTION OF THE GLOBAL PMSM SYSTEM

The figure 5 represents the total diagram of the vectorial command of a PMSM in a reference mark (d,q). The reference of the forward current I_d^* is fixed at zero and the output of the speed regulator I_q^* constitutes the instruction of the torque.

The forward reference currents I_d^* and I_q^* are compared separately with the real currents I_d and I_q of the motor. The errors are applied to the input of the traditional PI regulators. A decoupling block generates the standards reference voltage V_d^*, V_q^*. The system is provided with a regulation speed loop which makes it possible to generate the reference of current I_q^*. This reference is limited to the maximum current. On the other hand, the forward reference current I_d^* is imposed null in our case.

The outputs of the currents regulators I_d and I_q in the reference mark (a, b, c) are used as references of the voltage $\left(V_a^*, V_b^*, V_c^*\right)$ for the inverter control which feeds the PMSM.

From the matrix form (13) we pose: $U_d = V_d + e_d$, $U_q = V_q + e_q$ and $p = \frac{d}{dt}$ the differential operator, with $e_d(p) = \omega L_q . i_q$ and $e_q(p) = -\omega L_d i_d + \omega\phi_f$. We can write the following transfer function:

$$F_d(p) = \frac{I_d(p)}{V_d(p) + e_d(p)} = \frac{1}{R_a + p L_d} \tag{20}$$

$$F_q(p) = \frac{I_q(p)}{V_q(p) + e_q(p)} = \frac{1}{R_a + p L_q} \tag{21}$$

The compensation causes to uncouple the two axes thanks to a reconstitution in real time from these reciprocal disturbances $\left(e_d(p) \text{ et } e_q(p)\right)$. Under such conditions, the system becomes linear, we obtain:

$$V_d' = V_d + \omega L_q . i_q = \left(R_a + p L_d\right) i_d \tag{22}$$

$$V_q' = V_q - \omega L_d . i_d - \omega \phi_f = \left(R_a + p L_q\right) i_q \tag{23}$$

Therefore the two axes are well uncoupled; the axis d does not depend to any more an axis q .

Thus,

$$V_d^* = V_d' - \omega L_q . i_q \tag{24}$$

$$V_q^* = V_q' + \omega L_d . i_d + \omega \phi_f \tag{25}$$

For a damping coefficient, for PMSM, $\xi = 0.7$, and $\omega_n . t_{rep} = 3$, t_{rep}, representing the response time of speed, the transfer functions for current i_d and current i_q of the system in open loop are respectively, (Fig. 5).

$$H_d(p) = C_d(p) \times \left(G_0 / R_S / \left(1 + \tau_d p\right)\right) \tag{26}$$

$$H_q(p) = C_q(p) \times \left(G_0 / R_S / \left(1 + \tau_q p\right)\right) \tag{27}$$

with $\tau_d = \frac{R_S}{L_d}$ and $\tau_q = \frac{R_S}{L_q}$.

The proportional-integral regulators PI $\left(C_d(p)\, C_q(p)\right)$, whose transfer functions are given by:

$$C_d(p) = C_p(q) = K\left(1 + \tau_d p\right)/p\left(\ C_q(p)\right) \tag{28}$$

with: $K = R_S / \left(2 . G_0 . T_S\right)$. G_0, T_S are gain coefficient and the sampling frequency.

7. ASYNCHRONOUS MOTOR MODEL

The mathematical dynamic model of the asynchronous motor is described by the equations set [8-11], [13]:

$$\frac{dI_{sd}}{dt} = \frac{1}{\sigma L_s}\left[-(R_a + \frac{M^2 R_r}{L_r^2}) I_{sd} + \omega_s \sigma L_s I_{sq} + \frac{M R_r}{L_r}\phi_{rd} + \frac{M}{L_r}\omega_m \phi_{rq} + V_{sd}\right] \tag{29}$$

$$\frac{dI_{sq}}{dt} = \frac{1}{\sigma L_s}\left[-(R_a + \frac{M^2 R_r}{L_r^2}) I_{sq} - \frac{M}{L_r}\omega_m \phi_{rd} + \frac{M R_r}{L_r}\phi_{rq} - \sigma\omega_s L_s I_{sd} + V_{sq}\right] \tag{30}$$

$$\frac{d\phi_{rd}}{dt} = \frac{-R_r}{L_r}\phi_{rd} + (\omega_s - \omega_m)\phi_{rq} + \frac{M R_r}{L_r} I_{sd} \tag{31}$$

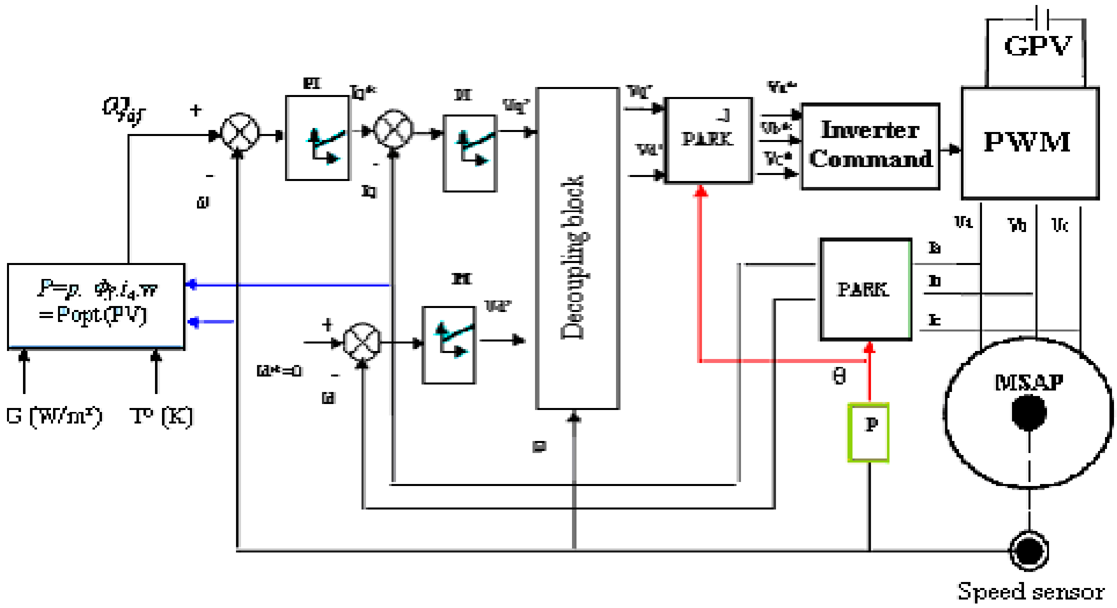

Fig. 5: Block diagram of the PMSM and the GPV

$$\frac{d\phi_{rq}}{dt} = \frac{-R_r}{L_r}\phi_{rq} - (\omega_s - \omega_m)\phi_{rd} + \frac{MR_r}{L_r} I_{sq} \tag{32}$$

$$J\frac{d\omega}{dt} = C_{em} - C_r \tag{33}$$

In this case, the ASM develop an electromagnetic torque Te expressed as follows:

$$C_{em} = \frac{M p_p^2}{L_r}(I_{sq}\phi_{rd} - I_{sd}\phi_{rq}) \tag{34}$$

d, q : axes corresponding to the synchronous reference frame. L_s, L_r, R_a, R_r and M are : stator and rotor main inductances, resistances and intrinsic self-inductance respectively. J is total inertia, σ dispersion factor. I_{sd}, ϕ_{rd}, I_{sq}, ϕ_{rq} are d-axis stator current, rotor flux and q-axis stator current, rotor flux respectively. ω_s and ω_m are the angular speed of the rotating magnetic and electric fields.

<u>AS Motor Characteristics</u>: $P = 746$ W ; $f = 60$ Hz ; $I_{sn} = 3.4$ A ; $C_{em} = 5$ N.m ; $R_a = 4\ \Omega$; $L_s = 0.3676$ H ; $R_r = 1.143\ \Omega$; $L_r = 0.3676$ H ; $M = 0.3439$ H ; $J = 3\ 10^{-2}\ kg/m^2$; $p_p = 2$.

8. GLOBAL ASM SYSTEM

For a damping coefficient, for ASM, $\xi = 1$, and $\omega_n . t_{rep} = 4.75$ s . t_{rep} representing the response time of speed. The transfer function for current i_{sd} and i_{sq} of the system in open loop is:

$$H(p) = C(p) \times \frac{1}{R_a(1 + \tau_s p)} \tag{35}$$

$$C(p) = K_p + \frac{K_i}{p} \tag{36}$$

with $\tau_s = \frac{R_a}{L_s}$. K_i and K_p the proportional-integral parameters.

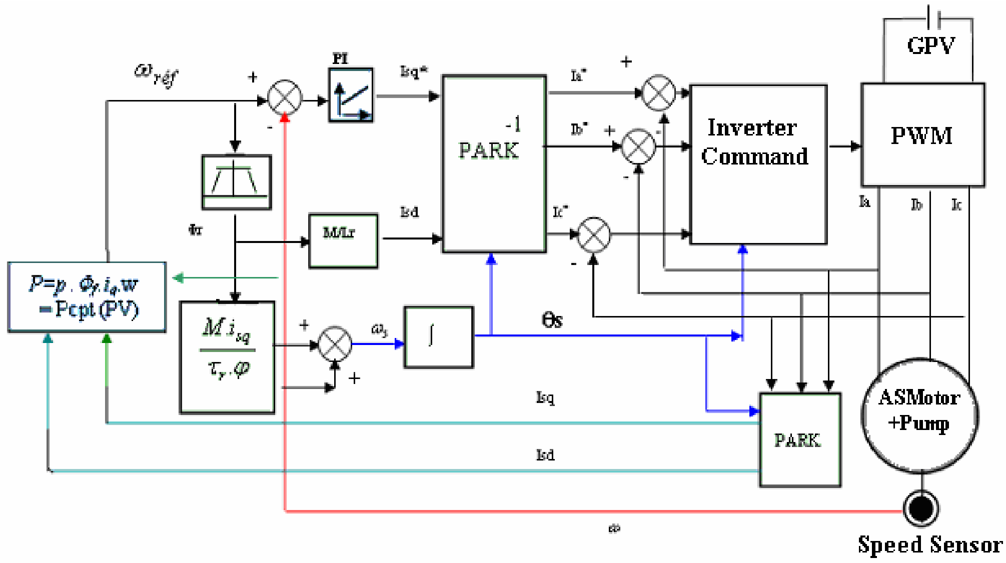

Fig. 6: Block diagram of an ASM vectorial command

9. SIMULATION RESULTS OF THE PMSM

For a referential speed $\left(\omega = \pm 200 \text{ rad/sec} \right)$ and starting from 0.3 s, the system is stabilized on the level of the reference variables (current and speed), the stator current $i_s = \pm 5$ A. Figures 7c and 7d shows that the d-axis current is null because it follows the reference d-axis current L_d supposed equal to zero according to the vectorial command principle {see paragraph 4 and equation (15)}. The q-axis current L_q is stabilized around 10 A, the couple electromagnetic being proportional to the q-axis current.

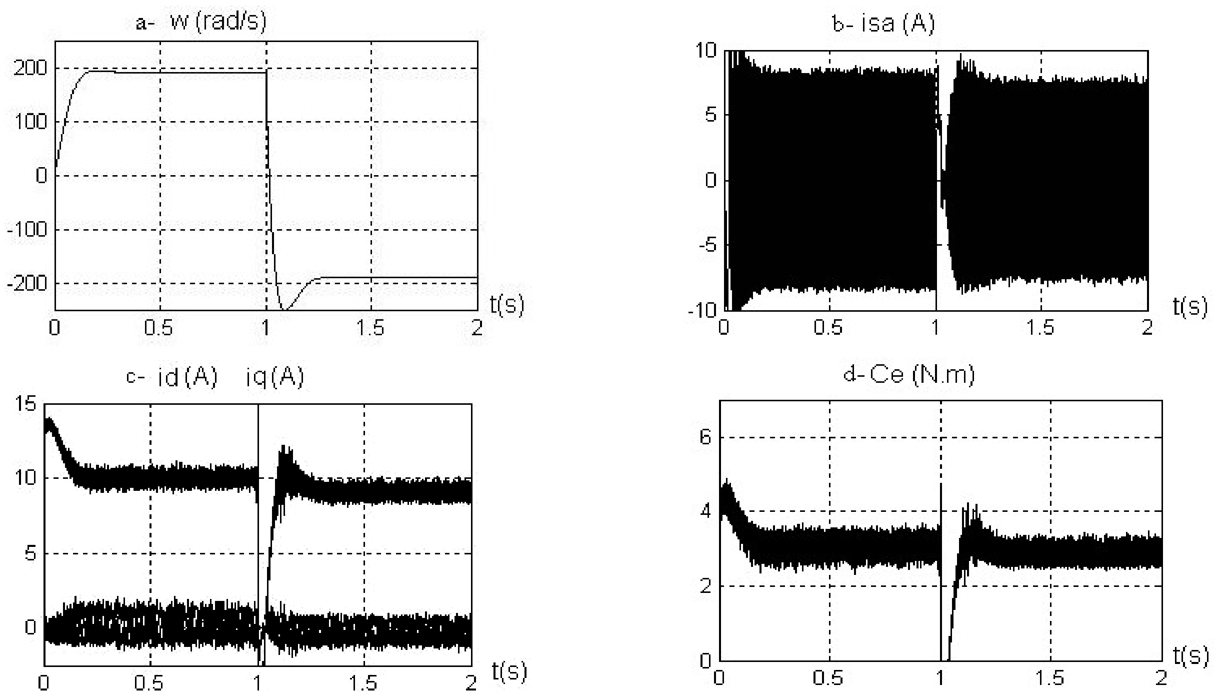

Fig. 7: Simulation results of speed, stator current per phase and motor torque

10. SIMULATION RESULTS OF THE ASM

For a referential speed $\left(\omega = \pm 200 \text{ rad/sec} \right)$ and starting from 0.5 s, the system is stabilized on the level of the reference variables (current and speed), the stator current $i_s = \pm 5$ A. It can be seen in Fig. 8b that the flux magnitude is constantly maintained and stays at a recommended value of 0.8 Wb.

Figures 8a and 8d shows the waveform of rotor speed, rotor flux, park reference stator current and stator current per phase. Also in spite of the step changes in the external load torque, the rotor speed and rotor flux tracking are successfully achieved. It is important to note that, even though the power provided by the photovoltaic generator is lower than its maximum, this result has motivated the use of DC/AC inverter for ensuring the desired maximum power point tracking, which essentially keeps the convergence power to its optimal value. In order to test the efficiency of the proposed method, we also carried out some simulations in the case that the photovoltaic generator is able to function around.

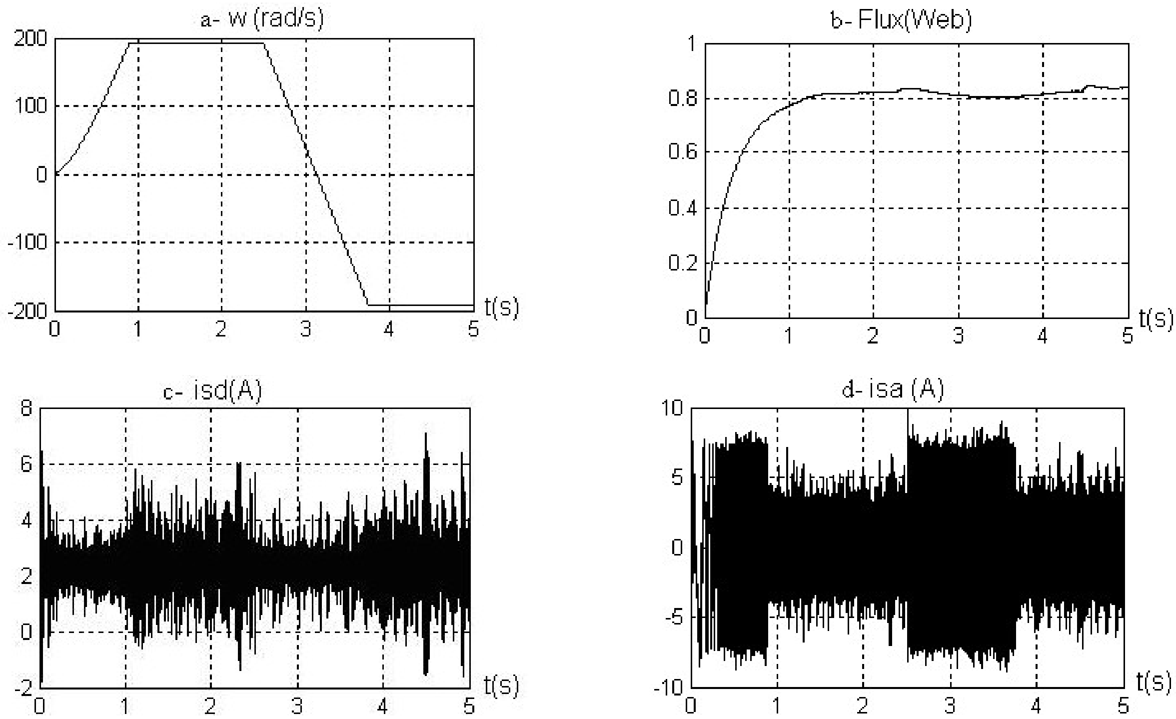

Fig. 8: Simulation results of speed, flux and statoric current

11. LOCATION OF MAXIMUM POWER POINTS

The generator power is equal to $P_{pv} = V_{pv} \times I_{pv}$ and the maximum power is obtained for:

$$\frac{\partial P_{pv}}{\partial V_{pv}} = \frac{\partial I_{pv}}{\partial V_{pv}} V_{pv} + I_{pv} = 0 \tag{37}$$

Let I_{mp} be the value of optimal current when power is maximum. By substituting $\frac{\partial I_{pv}}{\partial V_{pv}}$, V_{pv} and I_{pv} by their values in (37), we obtain the following equation:

$$I_{mp} + \frac{(I_{mp} - I_L - I_0).\left[Ln\left(\frac{I_L - I_{mp}}{I_0} + 1 \right) - \frac{I_{mp} R_S}{A} \right]}{1 + (I_L + I_{mp} + I_0) \frac{R_S}{A}} = 0 \tag{38}$$

The solution of the equation (38) by the Newton-Raphson method in motor-pump coupling mode, is governed by the following equation:

$$I_{mp} \times V_{mp} = p \cdot \phi \cdot \omega \cdot i_q \cdot \eta_c \cdot \eta_m \cdot \eta_p \tag{39}$$

η_c , η_m , η_p are respectively the inverter efficiency, motor efficiency and pump efficiency.

12. CENTRIFUGAL PUMP MODEL

The head-flow rate $H-Q$ characteristic of a monocellular centrifugal pump is obtained using Pleider-Peterman model [14, 15]. The multispeed family head-capacity curves are shown in figure 9 and can be expressed approximately by the following quadratic form:

$$h = a_0\,\omega_r^2 - a_1\,\omega_r\,Q - a_2\,Q^2 \tag{40}$$

with a_0, a_1, a_2 are coefficients given by the manufacturer.

The hydraulic power and the resistive torque are given by:

$$P_H = \rho\ g\ Q\ H \tag{41}$$

$$C_r = k_r\,\Omega^2 + C_s \tag{42}$$

Q : Water flow (m^3/sec), H : Manometric head of the well (m).

Centrifugal pump parameters: $\omega_n = 150\ \text{rad/sec}$; $a_1 = 4.9234\ 10^{-3}\ \text{m}/(\text{rad/sec})^2$;

$a_2 = 1.5826\ 10^{-5}\ \text{m}/(\text{rad/sec})(\text{m}^2/\text{sec})$; $a_3 = -18144\ \text{m}/(\text{m}^3/\text{sec})^2$

Canalisation parameters: $H = 10\ \text{m}$; $l = 7.4\ \text{m}$; $d = 0.006\ \text{m}$; $g = 9.81\ \text{m}^2/\text{sec}$; $\rho = 1000\ \text{kg/m}^3$

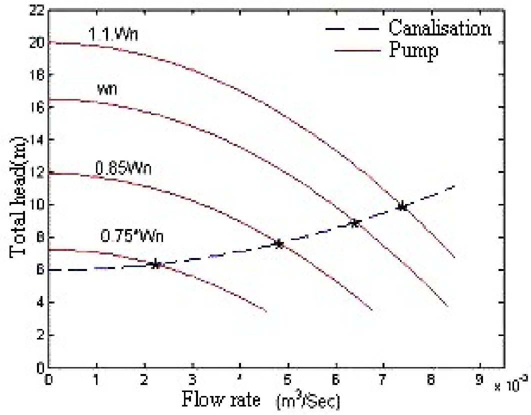

Fig. 9: Flow rate characteristics

13. ILLUMINATION'S INFLUENCE ON WORKING OPTIMAL POINT

While keeping the power generator at constant value, the optimization system improves the motor efficiency which will work around the working optimal point of the generator (Fig. 10).

The optimization system improves the motor efficiency which will work around the working optimal point of the generator; the load motor power characteristic will slip towards the band of the generator maximum powers, which ranges between 180 and 220 volts, for a variable illumination levels between 250 W/m^2 and 1100 W/m^2 (Fig. 11). For the direct coupling the driving system motor-pump functions only start from 250 W/m^2 for ASM and 300 W/m^2 for PMSM, contrary to the optimized coupling whose splashing phase ceases starting from 100 W/m^2 (Fig. 13 and 14). For a temperature $T = 298\ \text{K}$, and an illumination $G = 450\ \text{W/m}^2$, the power gain is 49.32 % for PMS Motor and 25.23 % for AS Motor, after optimization, it will be 20.12 % for PMSM and 7.35 % for ASM at 900 W/m^2. Optimization is better for weak illuminations, until $600\ \text{W/m}^2$, the global efficiency of the complete system generator, motor-pump being weak, approximately between 7 % and 8 %.

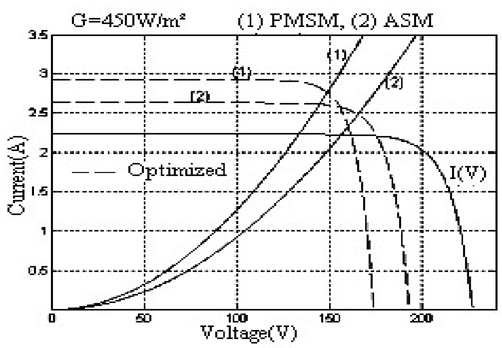

Fig. 10: I-V and load characteristics

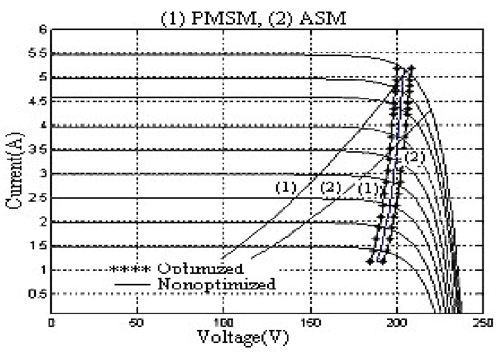

Fig. 11: Operation points of the PV pumping

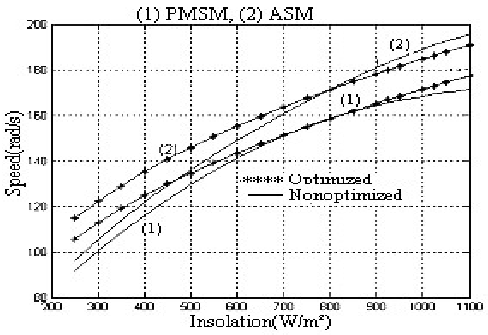

Fig. 12: Speeds of PV pumping driven by PMSM (1) and an ASM (2)

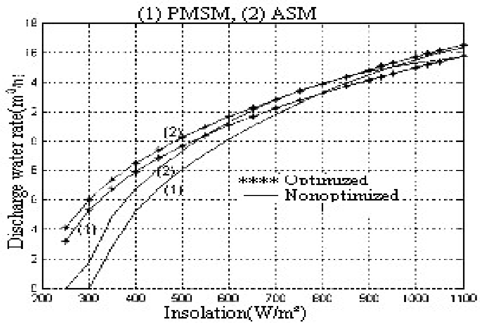

Fig. 13: Flow rate of PV pumping

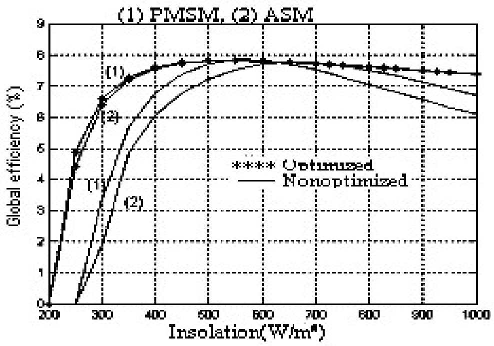

Fig. 14: Global efficiency of PV pumping

14. CONCLUSION

We showed the principal characteristics of a photovoltaic system allowing the pumping of water with solar energy. A PV generator outputting on an electronic power inverter detecting the working optimal point is presented. This generator drives a synchronous permanent magnet motor with smooth poles firstly and an induction motor that by using the vectorial command principle in the reference (d, q). This method makes it possible to obtain very good performances similar to those of a DC motor, because one obtains an electromagnetic torque directly proportional to the current absorptive by the load.

For achieving better motor torque generating characteristics, the conventional PI controller has been introduced in this paper for the vectorial command of an ASM machine fed by a photovoltaic generator. A current control scheme combining a decoupling control to achieve a fast dynamic response in a field orientation-controlled induction motor drive was presented in this paper. The ASM machine drive with rotor flux, stator current and speed controllers has exhibited good transient and steady-state performance. The results show the flux magnitude has been maintained as constant and a torque exhibits a fast response.

In this paper to take advantage of the field oriented-control, the flux and current controller have been designed using stator and rotor equations in the rotor flux frame since the flux and current controllers have simple forms according to the choice of closed-loops transfer functions, they can be easily designed and implemented. On the other hand, the control of the duty ratio is achieved by using the integral controller. The use of this controller gives good results for the maximum power tracking.

A comparative study was carried out on the systems described in Mimouni *et al.* [16] and Duzat [17]. The simulation results show that an increase of both the daily pumped quantity and pump efficiency are reached by the proposed approach. In addition, the generator voltages control law leads to a less expensive and noncomplex implementation. Thus the advantages described are acquired meanwhile overriding their inconvenience.

NOMENCLATURE

E_q	Band gap energy (eV)	q	Electronic charge (C)
G	Insolation (W/m^2)	Q	Flow rate (m^3/sec)
H	Total head (m)	R_a	Statoric resistance per phase (Ω)

H_g	Geodetic head (m)	R_r	Rotoric resistance per phase (Ω)
I_D	Reverse saturation current (A)	R_S	Series resistance of PV cell (Ω)
I_{mp}	Maximum point current (A)	V_{pv}	Output generator voltage (V)
I_{pv}	Generator current (A)	V_{mp}	Maximum point voltage (V)
I_{sc}	Short-circuit current (A)	V_{oc}	Open circuit voltage (V)
k	Boltzmann's constant (J/K)	V_S	Motor voltage (V)
L_d	d-axis self inductance of the stator (H)		***Greek symbols***
L_q	q-axis self inductance of the stator (H)	η_c	Cell efficiency
T_{noct}	Nominal Operating Cell Temperature	$\mu_{I_{sc}}$	Temperature coefficient of short-circuit current (A/°C)
n_s	Number of cells in series and in parallel	$\mu_{V_{oc}}$	Temperature coefficient of open circuit voltage (V/°C)
P_{max}	Maximum power of PV panel (W)	ρ	Water volumic mass (kg/m^3)
p_p	Number of pole pairs	τ_α	Transmittance absorbance product
M	Mutual inductance (H)	ω	Motor speed (rad/s)

REFERENCES

[1] J. Appelbaum and J. Bany, '*Performance Characteristics of a Permanent Magnet DC Motor Powered by Solar Cells*', Solar Energy, 22, p. 439, 1979.

[2] J. Appelbaum and M.S. Sharma, '*The Operation of Permanent Magnet DC Motors Powered by a Common Source of Solar Cells*', IEEE Trans. Energ. Convers., 4, pp. 635 – 642, 1989.

[3] J.A. Roger, '*Theory of the Direct Coupling between DC Motors and Photovoltaic Solar Arrays*', Solar Energy, 23, p. 193, 1979.

[4] W. Anis and H.M.B. Metwally, '*Dynamic Performance of a Directly Coupled PV Pumping System*', Solar Energy, 53, 3, 1994.

[5] A. Betka and A. Moussi, '*Performance Optimization of a Photovoltaic Induction Motor Pumping System*', Renewable Energy, 29, pp. 2167 – 2181, 2004.

[6] C. Hua, J. Lin and C. Shen, '*Implementation of a DSP Controlled Photovoltaic System with Peak Power Tracking*', IEEE Trans. Ind. Electronics, Vol. 45, N°1, pp. 99 - 107, Feb. 1998.

[7] E. Muljadi, '*PV Water Pumping with a Peak Power Tracker using a Simple Six Step Square-Wave Inverter*', IEEE Trans. Industry Applications, Vol. 33, N°3, pp. 714 - 721, May/June 1997.

[8] M.F. Mimouni, R. Dhifaoui, J.F. Brudny and D. Roger, '*Field-Oriented Control of Double-Star Induction Machine*', Int. Journal System of Analysis Modelling Simulation, (SAMS), 37, pp. 181 – 202, 2000.

[9] G. Grellet et G. Clerc, '*Actionneurs Electriques - Principes Modèles Commande*', Eyrolles, 1997.

[10] B.K. Bose, '*A High Performance Inverter – Fed Drive System of Interior Permanent Magnet Synchronous Machine*', IEEE Trans. Appl., Vol Ia-24, pp. 97 - 997, Nov/Dec 1998.

[11] T.M. Jahns, '*Flux – Weakening Regime Operation of an Interior Permanent Magnet Synchronous motor Drive*', IEEE on IA , Vol Ia, N°4, pp. 681 - 689, July/Aug 1987.

[12] J.M. Kin and S.K. Sul, '*Speed Control of Interior Permanent Magnet Synchronous Motor Drive for Flux Zeaking Operation*', 3in Proc. IEEE IAS Annuel: eet mpp. pp. 216 - 221, 1995.

[13] J.M.D. Murphy and F.G. Turnbull, '*Power Electronics Control of AC Motors*', Pergamon Press, 1985.

[14] A. Hamidat, A. Hadj Arab, F. Chenlo and M.A. Abella, '*Performances Costs of the Centrifugal and Displacement Pumps*', WREC, pp. 1951 – 1954, 1998.

[15] A. Moussi, A. Betka and B. Azoui, '*Optimum Design of Photovoltaic Pumping System*', UPEC99, Leicester, UK, 1999.

[16] M.F. Mimouni, M.N. Mansouri, B. Benghanem and M. Annabi, '*Vectorial Command of an Asynchronous Motor Fed by a Photovoltaic Generator*', Renewable Energy, 29, pp. 433 – 442, 2004.

[17] R. Duzat, '*Analytic and Experimental Investigation of a Photovoltaic Pumping System*', PhD Thesis, Oldenburg University, 2000.